161.06 / W17

Characterizing resonant and synchronizing mechanisms in a hippocampal theta model

Tyler Banks[1],Vinay Guntu[1], Ali Hummos[2], Satish S Nair[1]
[1]Department of Electrical and Computer Engineering, University of Missouri, Columbia, MO
[2] Department of Health Informatics, University of Missouri, Columbia, MO

Introduction

- Hippocampal theta oscillations (4–12 Hz) are consistently recorded during memory tasks and spatial navigation. [1]
- Our previous model generated theta power robustly through five cooperating generators [2]. Here we distinguish between resonant components and synchronizing components of theta generators.
- **Resonant mechanisms** inherently produce rhythmic signals as a product of their dynamics and include spike-frequency adaptation, slow inhibition, rhythmic external inputs and slow neuronal currents.
- **Synchronizing mechanisms** promote coordinated activity and include inhibitory feedback, non-rhythmic external input and recurrent excitatory connections.
- Some circuit components can provide both resonance and synchronization. Ex: Rhythmic external input and Excitatory to Slow Inhibition connections.
- Our goal is to examine interaction between circuit components that participate in theta rhythm generation in CA3.

Network/ Methods

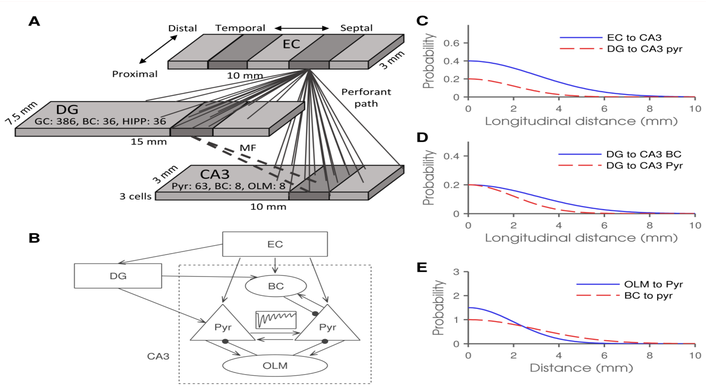

Fig(1): Network 3D structure and CA3 local circuitry [3]

(A) Schematic of the network implemented showing the modeled regions EC, CA3, and DG with their dimensions, cell numbers, and lamellar connectivity pattern. Neurons in EC are more likely to send connections to DG and CA3 neurons in their longitudinal vicinity. Similarly, DG granule cells in the same longitudinal neighborhood are likely to project to CA3 neurons in the same lamella. Cells were compacted into three sheets of cells, in the radial dimension, representing stratum-pyramidale in CA3 and the granular layer in DG.

(B) Schematic with details of CA3 internal circuitry. Excitatory connections terminate in arrows and inhibitory ones in black filled circles.

(C) Gaussian connection probability functions. The longitudinal organization of EC inputs to CA3 is compared to DG inputs. Inputs from DG had a more focused pattern of connectivity.

(D) Projections from MF to BCs had a wider longitudinal extent, compared to the ones from MF to CA3 pyramidal cells (pyr).

(E) The probability of an interneuron connecting to a pyramidal cell depended on the distance between the two in the longitudinal and transverse planes. Note that probability for the OLM domain exceeded one to ensure that OLM cells made dense connections in their immediate neighborhood.

- **Single cell models**: developed using the Izhikevich formulation [4]. The equations for a model neuron were as follows:

$$\frac{dv}{dt} = -k(v - v_t)(v - v_r) - u + h + I;\ \frac{du}{dt} = -a\{b(v - v_r) - u\};\ if\ v > vpeak\ then\ v = c\ and\ u = u + d$$

H-current : $\frac{dh}{dt} = -a_h(b_h(v - v_r) - h)$

where v is the membrane potential of the cell, u is a recovery variable, vt is the 'instantaneous threshold' beyond which the cell will fire an action potential, vr is the resting membrane potential, I is the current injection, k is a constant used to adjust the input resistance and rheobase, vpeak is the threshold above which a spike is deemed to have occurred and the membrane potential is reset, and a, b, c, and d are parameters used to tune the behavior of the system to model the neuro-computational properties of the desired cell. h is the h-current value, and a_h, b_h are parameters used to tune the behavior of the pyr and OLM cells.

- **Synaptic currents**: AMPA, NMDA, $GABA_A$, and $GABA_B$ currents were modeled and their dynamics such as rise and decay time constants and delays were matched to available literature [3]
- **Activity-dependent plasticity**: For this study, long-term plasticity was excluded from the synapses. Model synapses, however, exhibited short-term synaptic plasticity.
- **Acetylcholine effects**: To implement the effects of ACh on model neurons and synapses, w e used a variable 'ACh' to represent the ACh state. The variable ACh had values of 0 (low), 1 (baseline), and 2 (high). Cholinergic stimulation has differential effects on synaptic transmission of different pathways in the hippocampus and enhanced cellular excitability and depolarized the resting membrane potential of principal cells, eliminated AHP, decreased spike frequency adaptation and induced rhythmic burst activity.
- **Inputs**: For the full model and sub-circuit cases considered, either EC cells or CA3 pyramidal cells (figures(2,3)) received external input as trains of Poisson-distributed spikes. We studied two model cases: one with external input arriving at EC, and the other with input arriving directly at CA3 pyramidal cells. To determine the base rates of the Poisson processes generating these input trains, we considered place cells in CA3. Place cells respond to certain areas in the environment and their firing rates approximate a lognormal distribution with an average of ~7 Hz [5] . A constant current injection was added to the voltage equation and the current amplitude was adjusted to maintain the physiologically reported average firing rate and lognormal distribution of firing rates.
- **Data analysis**: we summed the spikes of all cells of each type in a region (e.g., CA3 pyramidal cells) in 0.1 ms bins and computed the fast-Fourier transform of the resulting vector
- **Software's used**: NEURON (Model) and Matlab (Analysis)

Results/ Discussion

Fig (2): Multiple generators of theta oscillations in the hippocampal CA3 network [2].
(A-E) (1) Shows where inputs are provided, sub circuits activated, (2) spike raster plot of pyr cells, (3) power spectrum of pyr cells.

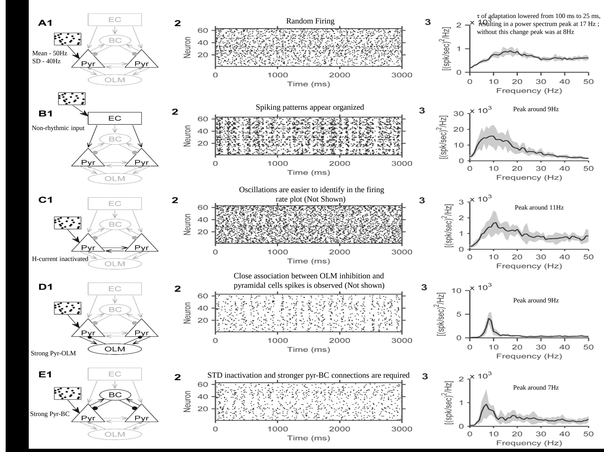

The model reproduced the physiological aspects of theta rhythmic activity in the hippocampus. [5]

✓ ***Multiple interacting mechanisms:***
We here used our model, with many theta generating components, to show a complex interaction between the component inactivated, other active components, in addition to the cholinergic state, to determine the effects of inactivation on the power spectrum.

our results are consistent with findings by Royer et al., 2012 [6] where optogenetic inactivation of either BCs or OLM did not impact theta generation significantly. In our model- in low cholinergic states, BCs and OLMs were able to compensate for one another to generate theta Fig (4.1A). However, our model predicts that in a high cholinergic state, the same experiment could show a dramatic drop in theta with OLM inactivation, and an increase in theta power with BCs inactivation Fig (4.1C).

✓ ***Resonant and synchronizing mechanisms act in concert to generate rhythms:***
Our work suggests that almost any interneuronal population, if reciprocally connected to pyramidal cells, can participate in rhythm generation, as a synchronizing component.

A contribution of our study was to examine effects of inactivating interneurons while maintaining excitation levels within physiological limits. We provided pyramidal cells with a constant current injection to offset the effects of inactivating inhibitory interneurons on level of excitation. Isolating effect of interneurons on excitation level, revealed their role in rhythm generation by acting as synchronizing mechanisms.
We here emphasized the role of the OLM-pyramidal cells sub-network in providing resonance in theta frequency, however OLM cells also do participate, as do many interneurons, as a synchronizing mechanism.

✓ ***Fast spiking basket cells as synchronizing component for theta generation:***
BCs can synchronize pyramidal cells spikes to a degree where BCs themselves begins to receive increasingly synchronized excitation from pyramidal cells, and in turn provides theta rhythmic inhibition, thus amplifying the rhythmic activity. Fig (2E)

✓ ***Competition and interference:***
The model predicts conditions were inactivation of a resonant or a synchronizing mechanism might enhance rhythmic activity, indicating that their presence interfered with other active generators.

Fig (3.1) Pyramidal cells slow currents and OLM-pyramidal cells loop are the two resonant mechanisms.
(A)The power spectra of 6 simulations. The 'None' experiment had no theta generating components with isolated pyramidal cells with no slow currents, and direct unique Poisson input with no correlations. The following experiments activated one theta component at a time and examined the power spectrum. The recurrent connections were activated in '+RC' and produced a small bump in the 2-4 Hz range. BCs activated in '+BC' produced no spectral peaks. Routing input through the EC added correlations in the external input and shift the power to low frequencies but did not produce theta peaks. *Adding OLM cells '+OLM' produced a robust theta peak. Activating the slow currents in pyramidal cells also produced a small but significant peak in theta frequencies* '+RES'.
B) relative theta calculations. '+RC', '+EC' increased relative theta due to a less specific increase in slow frequency power.
C) firing rates were kept within physiological range using the following current injections. None: 7 mA, +RC 8 mA, +BC 5 mA, +EC 10 mA, +OLM 1 mA, +RES 1 mA.

Fig (3.2) Resonant mechanisms can substitute for and compete with each other.
A) Schematic of this experiment with EC inactivated and input directly arriving at CA3 pyramidal cells. Both OLM cells, BCs, and the recurrent excitatory connections were active.
B) The power spectra of four experiments as follows: "full" simulated with both OLM cells and adaptation in pyramidal cells intact, "-OLM" was run with OLM cells inactivated, "-sPYR" had OLM cells intact but adaptation and h-current were removed from pyramidal cells, and finally "-both" had both pyramidal cells slow currents and OLM cells inactivated. *The power spectra indicate that theta activity persisted with at least one resonant mechanism intact, but also interestingly showed that pyramidal cells adaptation as a resonant component may have interfered with the OLM-pyramidal cells resonator.*
C) Relative power in the theta band (4-12 Hz) divided by total power (0-50 Hz) and normalized to the value of the "full" model run.
D) firing rates were kept within physiological range using the following current injections to pyramidal cells in the different experiments were as follows. Full: 3.5 mA, -OLM: 4.2 mA, -sPYR: 3 mA, -Both: 8.2 mA.

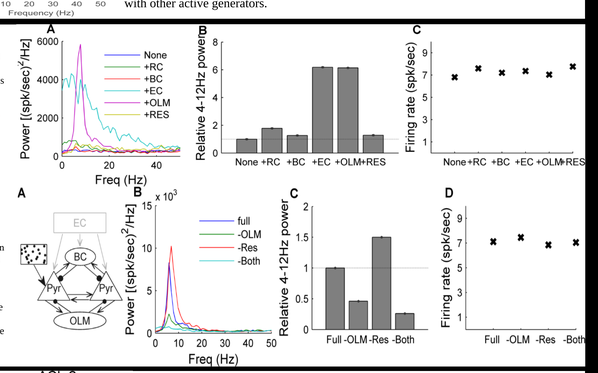

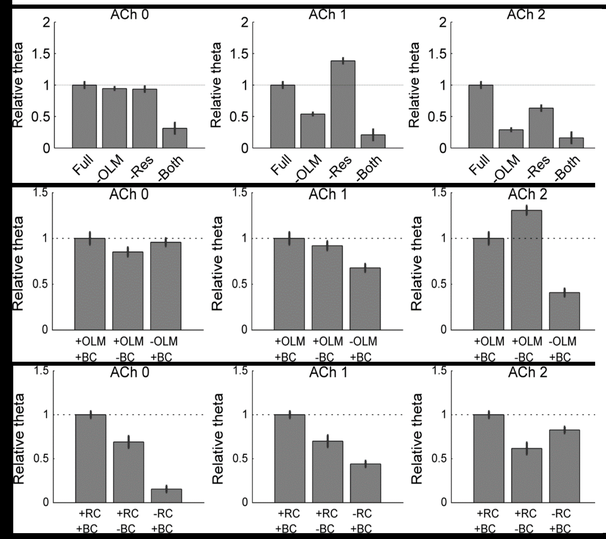

Fig (4.1) Functional separation at the extremes of cholinergic modulation minimizes interference between resonating mechanisms.
Current injections to compensate for variation in firing rates: ACh 0: Full: -2 mA, -OLM: -2 mA, -sPYR: 0 mA, -Both: 2 mA. ACh 1: Full: 3.5 mA, -OLM: 4.2 mA, -sPYR: 3 mA, -Both: 8.2 mA. ACh 2: Full: 4 mA, -OLM: 5 mA, -sPYR: 3.5 mA, -Both: 8.5 mA.

We found that there is a potential for interference between the two resonant mechanisms in our model. Different cholinergic states engage different theta mechanisms [2]. we theorized that by functionally separating the two mechanisms, cholinergic modulation might reduce the interference between the two resonant mechanisms. Examination of relative theta power in these conditions revealed that in the extremes of cholinergic modulation (low and high), the pattern of slow currents interfering with OLM generated theta disappeared .

Fig (4.2) Synchronizing mechanisms can substitute for or interfere with one another
Recurrent connections and EC were inactivated, leaving the two synchronizing mechanisms in the model, OLM cells and BC cells. We tested three conditions, first with both OLM and BC cells active (+OLM +BC), and then with BCs inactivated (+OLM -BC) and finally, with OLM cells inactivated (-OLM +BC). Current injections to compensate for variation in firing rates: ACh 0: +both: -7 mA, -BC: -6.5 mA, -OLM: -7.5 mA. ACh 1: +both: -3 mA, -BC: 1 mA, -OLM: -6.1 mA. ACh 2: +both: -1 mA, -BC: 2.8 mA, -OLM: 1.4 mA.

Running the three conditions under three different cholinergic states revealed different interaction modes between the two synchronizing mechanisms. In low ACh, they were equally effective at generating theta, and only one mechanism appeared necessary. With increasing cholinergic levels, BCs contribution to theta diminished, and in high cholinergic states they interfered with OLM generated theta.

Fig(4.3) Recurrent connections and BCs cooperatively synchronize theta oscillations.
OLM cells and EC were inactivated, leaving the two synchronizing mechanisms in the model, recurrent connections and BC cells. We tested three conditions, first with both recurrent connections and BC cells active (+RC +BC), and then with BCs inactivated (+RC -BC) and finally, with recurrent connections inactivated (-RC +BC). Current injections to compensate for variation in firing rates: ACh 0: +both: 5 mA, -BC: 6 mA, -RC: 1 mA. ACh 1: +both: 2 mA, -BC: 5 mA, -RC: -2 mA. ACh 2: +both: -2 mA, -BC: 5 mA, -RC: -2 mA

Running the three conditions under three different cholinergic states revealed a stable engagement of BCs in theta generation while recurrent connection had a stronger engagement in lower cholinergic states.

Limitations/Future Work

- Our model falls short of representing the diversity of theta generators and analyzing more complex interactions that involve a larger number of rhythm generators.
- Neuromodulators (such as endocannabinoids, and serotonin) have effects of theta generation and likely have a role in determining which theta generators are actively engaged.
- Analysis of the h-current can allow examination of its role specifically and separate from spike-frequency adaptation.
- We have developed an updated, functional model with biologically realistic cells using Allen Institute's BMTK and plan to reproduce previous plots.
- Model includes h-current but it remained mathematically difficult to separate from the adaptation current in pyramidal cells. A more realistic pyramidal cell model can allow examination of its role specifically and separate from spike-frequency adaptation.
- Another area of future interest would be to examine how individual theta generators interact with rhythmic external input. Results can vary from competition and interference to synergy.
- Combinations of intrinsic theta generators might also respond differently than individual ones.

Conclusions

- As a conceptual framework for hippocampal theta generation, we propose a useful distinction between resonant and synchronizing components.
- We found the most robust rhythm generation to require at least one resonant component and one synchronizing component.
- Pyramidal cells adaptation can interfere with theta produced by slow inhibition.
- Fast inhibition can either substitute for or interfere with rhythm generation by slow inhibition, depending on the cholinergic state.
- Effects of component inactivation can only be predicted in the context of what other components are present and on the neuromodulatory state of the circuit.
- These results begin to shed light on the conflicting evidence produced by studies inactivating circuit components, and also predicts circuit states where inactivating a component known to participate in rhythm generation might paradoxically enhance rhythmic activity.

References

1. Buzsáki, G. (2002). "Theta Oscillations in the Hippocampus." Neuron **33**(3): 325-340.
2. Hummos, A. and S. S. Nair (2017). "An integrative model of the intrinsic hippocampal theta rhythm." PLoS ONE **12**(8): e0182648.
3. Hummos, A., et al. (2014). "Intrinsic mechanisms stabilize encoding and retrieval circuits differentially in a hippocampal network model." Hippocampus **24**(12): 1430-1448.
4. E. M. Izhikevich, "Simple model of spiking neurons," in *IEEE Transactions on Neural Networks*, vol. 14, no. 6, pp. 1569-1572, Nov. 2003.
5. Mizuseki, K. and G. Buzsaki (2013). "Preconfigured, skewed distribution of firing rates in the hippocampus and entorhinal cortex." Cell Rep **4**(5): 1010-1021.
6. Royer, S., et al. (2012). "Control of timing, rate and bursts of hippocampal place cells by dendritic and somatic inhibition." Nat Neurosci **15**(5): 769-775.

Acknowledgement: This project was supported in part is supported by the NIH grant MH122023